

Supplementary materials for "The imbricated foreshock
and aftershock activities of the Balsorano (Italy) M_w
4.4 normal fault earthquake and implications for
earthquake initiation"

H. S. Sánchez-Reyes¹, D. Essing¹, E. Beaucé², P. Poli¹¹

¹*Institute of Earth Sciences, University Grenoble Alpes, Grenoble 38100, France*

²*Department of Earth, Atmospheric, and Planetary Sciences, Massachusetts Institute of
Technology, Cambridge, MA, United States*

^{*}*Corresponding author: hugo.sanchez-reyes@univ-grenoble-alpes.fr*

Contents of this file

1. Tables S1 to S4

2. Figures S1 to S2

Additional Supporting Information

1. Seismic catalog for the seismic sequence associated to the 2019 (M_W 4.4) Balsorano
earthquake

Table S1: General information of the 2019 M_w 4.4 Balsorano earthquake. All this information is taken from the INGV's online catalog.

| Mainshock data | |
|--------------------------|----------------------|
| Magnitude | M_w 4.4 |
| Lat (°) / Lon (°) | 13.61 / 41.78 |
| Depth (km) | 14.0 |
| NP1: Strike / Dip / Rake | 299 / 58 / -120 |
| NP2: Strike / Dip / Rake | 166 / 42 / -51 |
| Reported activity | \approx 150 events |
| # Stations < 100 km | 6 |

Table S2: Receiver locations. The distances reported are measured with respect to the mainshock epicentral location (taken from the INGV).

| Receiver | Lon. (°) | Lat. (°) | Dist. (km) |
|----------|----------|----------|------------|
| CERT | 41.94903 | 12.98176 | 72.297 |
| GUAR | 41.79450 | 13.31229 | 33.093 |
| INTR | 42.01154 | 13.90460 | 41.820 |
| POFI | 41.71743 | 13.71202 | 13.112 |
| PTQR | 42.02193 | 13.40057 | 35.780 |
| VVLD | 41.86965 | 13.62324 | 10.411 |

Table S3: Velocity model used for the relocation process. A V_P/V_S ratio equal to 1.73 is assumed. Slightly modified version from the model proposed by [Bagh et al. \(2007\)](#)

| Depth of top of layer (km) | P-wave velocity (km/s) |
|----------------------------|------------------------|
| 0.0 | 5.360 |
| 3.0 | 5.360 |
| 6.0 | 5.800 |
| 14.0 | 6.650 |
| 25.0 | 6.900 |

Table S4: Reference templates and phase traveltimes at the six available stations (estimated from INGV data).

| # | Origin time | P_{tt} | | P_{tt} | | P_{tt} | | P_{tt} | | P_{tt} | | S_{tt} | | S_{tt} | | S_{tt} | | S_{tt} | |
|----|---------------------|----------|------|----------|------|----------|------|----------|------|----------|------|----------|------|----------|------|----------|------|----------|------|
| | | CERT | GUAR | INTR | POFI | PTQR | VVLD | CERT | GUAR | INTR | POFI | PTQR | VVLD | CERT | GUAR | INTR | POFI | PTQR | VVLD |
| 1 | 2019/11/07 00:37:18 | 9.63 | 5.51 | 6.9 | 3.46 | 6.37 | 3.48 | 17.09 | 9.11 | 11.95 | 5.82 | 11.28 | 5.71 | 17.09 | 9.11 | 11.95 | 5.82 | 11.28 | 5.71 |
| 2 | 2019/11/07 03:21:00 | 9.72 | 5.38 | 6.92 | 3.57 | 6.62 | 3.57 | 17.15 | 9.4 | 12.12 | 5.87 | 11.36 | 5.82 | 17.15 | 9.4 | 12.12 | 5.87 | 11.36 | 5.82 |
| 3 | 2019/11/07 10:37:05 | 9.69 | 5.39 | 6.93 | 3.7 | 6.52 | 3.54 | 17.15 | 9.15 | 12.05 | 6.00 | 11.38 | 5.82 | 17.15 | 9.15 | 12.05 | 6.00 | 11.38 | 5.82 |
| 4 | 2019/11/07 17:35:21 | 9.7 | 5.38 | 7.01 | 3.54 | 6.48 | 3.59 | 17.22 | 9.02 | 12.12 | 5.89 | 11.52 | 5.92 | 17.22 | 9.02 | 12.12 | 5.89 | 11.52 | 5.92 |
| 5 | 2019/11/07 17:47:53 | 9.77 | 5.4 | 6.93 | 3.32 | 6.53 | 3.55 | 17.29 | 9.12 | 12.07 | 5.45 | 11.42 | 5.68 | 17.29 | 9.12 | 12.07 | 5.45 | 11.42 | 5.68 |
| 6 | 2019/11/07 18:04:55 | 9.74 | 5.35 | 6.9 | 3.39 | 6.54 | 3.49 | 17.21 | 9.12 | 11.86 | 5.68 | 11.45 | 5.72 | 17.21 | 9.12 | 11.86 | 5.68 | 11.45 | 5.72 |
| 7 | 2019/11/07 23:19:50 | 9.62 | 5.29 | 7.09 | 3.54 | 6.44 | 3.55 | 16.89 | 8.99 | 12.19 | 6.00 | 11.20 | 5.79 | 16.89 | 8.99 | 12.19 | 6.00 | 11.20 | 5.79 |
| 8 | 2019/11/08 03:08:06 | 9.06 | 5.14 | 7.06 | 3.56 | 6.45 | 3.42 | 16.85 | 8.76 | 12.21 | 5.85 | 11.08 | 5.58 | 16.85 | 8.76 | 12.21 | 5.85 | 11.08 | 5.58 |
| 9 | 2019/11/08 08:10:56 | 9.93 | 5.56 | 6.75 | 3.17 | 6.72 | 3.37 | 17.33 | 9.23 | 11.69 | 5.39 | 11.58 | 5.48 | 17.33 | 9.23 | 11.69 | 5.39 | 11.58 | 5.48 |
| 10 | 2019/11/08 08:16:10 | 9.84 | 5.44 | 6.88 | 3.44 | 6.51 | 3.54 | 17.40 | 9.49 | 12.00 | 5.76 | 11.53 | 5.71 | 17.40 | 9.49 | 12.00 | 5.76 | 11.53 | 5.71 |
| 11 | 2019/11/08 10:43:24 | 9.50 | 5.15 | 6.89 | 3.32 | 6.29 | 3.38 | 17.00 | 8.91 | 12.08 | 5.78 | 11.19 | 5.61 | 17.00 | 8.91 | 12.08 | 5.78 | 11.19 | 5.61 |
| 12 | 2019/11/08 12:00:43 | 9.75 | 5.44 | 7.04 | 3.34 | 6.61 | 3.55 | 17.29 | 9.13 | 12.44 | 5.70 | 11.35 | 5.77 | 17.29 | 9.13 | 12.44 | 5.70 | 11.35 | 5.77 |
| 13 | 2019/11/08 13:07:07 | 9.41 | 5.08 | 6.86 | 3.32 | 6.22 | 3.34 | 16.88 | 8.77 | 12.31 | 5.64 | 11.04 | 5.45 | 16.88 | 8.77 | 12.31 | 5.64 | 11.04 | 5.45 |
| 14 | 2019/11/08 14:22:12 | 9.52 | 5.14 | 6.92 | 3.39 | 6.48 | 3.38 | 16.99 | 8.79 | 12.39 | 5.69 | 11.19 | 5.56 | 16.99 | 8.79 | 12.39 | 5.69 | 11.19 | 5.56 |
| 15 | 2019/11/09 10:57:09 | 9.72 | 5.35 | 6.87 | 3.21 | 6.54 | 3.46 | 17.20 | 9.03 | 11.98 | 5.52 | 11.33 | 5.70 | 17.20 | 9.03 | 11.98 | 5.52 | 11.33 | 5.70 |
| 16 | 2019/11/09 22:14:15 | 9.59 | 5.27 | 6.66 | 3.24 | 6.43 | 3.14 | 17.07 | 9.04 | 11.61 | 5.33 | 10.91 | 5.04 | 17.07 | 9.04 | 11.61 | 5.33 | 10.91 | 5.04 |
| 17 | 2019/11/09 23:09:52 | 9.79 | 5.49 | 6.90 | 3.62 | 6.61 | 3.59 | 17.48 | 9.12 | 11.88 | 5.69 | 11.66 | 5.91 | 17.48 | 9.12 | 11.88 | 5.69 | 11.66 | 5.91 |
| 18 | 2019/11/10 03:31:36 | 9.55 | 5.15 | 6.58 | 3.51 | 6.37 | 3.42 | 16.82 | 8.68 | 12.21 | 5.79 | 11.07 | 5.55 | 16.82 | 8.68 | 12.21 | 5.79 | 11.07 | 5.55 |
| 19 | 2019/11/10 06:56:28 | 9.62 | 5.15 | 6.56 | 3.15 | 6.40 | 3.07 | 17.04 | 9.04 | 11.92 | 5.42 | 11.39 | 5.09 | 17.04 | 9.04 | 11.92 | 5.42 | 11.39 | 5.09 |
| 20 | 2019/11/11 01:43:21 | 9.59 | 5.31 | 6.90 | 3.44 | 6.42 | 3.53 | 18.00 | 9.27 | 12.05 | 5.25 | 11.44 | 5.76 | 18.00 | 9.27 | 12.05 | 5.25 | 11.44 | 5.76 |
| 21 | 2019/11/11 13:41:33 | 9.46 | 5.11 | 7.00 | 3.49 | 6.22 | 3.39 | 16.81 | 8.79 | 12.20 | 5.85 | 11.10 | 5.54 | 16.81 | 8.79 | 12.20 | 5.85 | 11.10 | 5.54 |
| 22 | 2019/11/11 16:04:53 | 9.39 | 5.05 | 6.95 | 3.43 | 6.25 | 3.34 | 17.07 | 8.70 | 12.27 | 5.75 | 11.08 | 5.52 | 17.07 | 8.70 | 12.27 | 5.75 | 11.08 | 5.52 |
| 23 | 2019/11/11 17:46:53 | 9.61 | 5.22 | 6.86 | 3.32 | 6.40 | 3.43 | 17.05 | 8.97 | 12.44 | 5.22 | 11.23 | 5.62 | 17.05 | 8.97 | 12.44 | 5.22 | 11.23 | 5.62 |

Table S5: Velocity model used for the relocation process. A V_P/V_S ratio equal to 1.73 is assumed. Slightly modified version from the model proposed by [Bagh et al. \(2007\)](#)

| ID | Orig. time | Lon. (hh) | Lat. (hh) | Depth (hh) | Est. Mag. | INGV Lon. | INGV Lat. | INGV Depth | INGV Mag. |
|-----|---------------------|-----------|-----------|------------|-----------|-----------|-----------|------------|-----------|
| 45 | 2019-11-07 00:37:18 | 13.6061 | 41.7737 | 13.972 | 1.1734 | 13.6082 | 41.7778 | 14.2 | 1.2 |
| 85 | 2019-11-07 03:21:00 | 13.6026 | 41.7744 | 13.87 | 1.3777 | 13.6117 | 41.7767 | 15.2 | 1.4 |
| 153 | 2019-11-07 10:37:05 | 13.6039 | 41.7735 | 13.862 | 1.3494 | 13.6047 | 41.7775 | 15.6 | 1.3 |
| 166 | 2019-11-07 17:35:21 | 13.6066 | 41.7746 | 13.94 | 4.2453 | 13.6043 | 41.7762 | 16.2 | 4.4 |
| 180 | 2019-11-07 17:47:53 | 13.6054 | 41.7747 | 13.809 | 2.2965 | 13.6117 | 41.7667 | 13.4 | 2.2 |
| 190 | 2019-11-07 18:04:55 | 13.6041 | 41.7739 | 14.357 | 1.4569 | 13.6128 | 41.7773 | 14.3 | 1.4 |
| 274 | 2019-11-07 23:19:50 | 13.6066 | 41.7812 | 13.713 | 3.4788 | 13.5967 | 41.777 | 15.1 | 3.5 |
| 357 | 2019-11-08 03:08:06 | 13.608 | 41.7778 | 14.172 | 1.4845 | 13.5908 | 41.7643 | 14.4 | 1.6 |
| 423 | 2019-11-08 08:10:56 | 13.6048 | 41.7753 | 14.159 | 1.5235 | 13.6287 | 41.778 | 12.7 | 1.5 |
| 425 | 2019-11-08 08:16:10 | 13.6065 | 41.7704 | 14.95 | 1.6368 | 13.6192 | 41.7772 | 14.9 | 1.6 |
| 433 | 2019-11-08 10:43:24 | 13.6053 | 41.7802 | 13.877 | 2.8811 | 13.5903 | 41.78 | 12.8 | 2.6 |
| 442 | 2019-11-08 12:00:43 | 13.6088 | 41.7767 | 14.029 | 1.1587 | 13.6063 | 41.766 | 14 | 1.1 |
| 448 | 2019-11-08 13:07:07 | 13.6056 | 41.7811 | 13.719 | 1.7611 | 13.5973 | 41.7817 | 12.7 | 1.8 |
| 453 | 2019-11-08 14:22:12 | 13.6035 | 41.7754 | 13.891 | 1.3305 | 13.5997 | 41.773 | 12.6 | 1.3 |
| 539 | 2019-11-09 10:57:09 | 13.601 | 41.7801 | 13.947 | 1.1306 | 13.6097 | 41.7755 | 13.6 | 1.1 |
| 540 | 2019-11-09 22:14:15 | 13.6147 | 41.7847 | 11.5 | 1.296 | 13.6147 | 41.7847 | 11.5 | 1.3 |
| 576 | 2019-11-09 23:09:52 | 13.605 | 41.7752 | 14.298 | 1.2884 | 13.6203 | 41.7737 | 15.2 | 1.4 |
| 597 | 2019-11-10 03:31:36 | 13.605 | 41.7795 | 14.343 | 1.3393 | 13.6018 | 41.7775 | 13.2 | 1.4 |
| 613 | 2019-11-10 06:56:28 | 13.6069 | 41.7713 | 15.211 | 1.4618 | 13.6055 | 41.7857 | 10.8 | 1.5 |
| 644 | 2019-11-11 01:43:21 | 13.6051 | 41.779 | 13.564 | 1.8014 | 13.6125 | 41.7682 | 13.5 | 1.7 |
| 658 | 2019-11-11 13:41:33 | 13.6058 | 41.7765 | 13.852 | 1.6433 | 13.5912 | 41.7768 | 13.1 | 1.7 |
| 665 | 2019-11-11 16:04:53 | 13.6076 | 41.779 | 13.805 | 1.5086 | 13.5938 | 41.7767 | 12.9 | 1.7 |
| 674 | 2019-11-11 17:46:53 | 13.6052 | 41.772 | 12.6 | 1.2764 | 13.6052 | 41.772 | 12.6 | 1.2 |

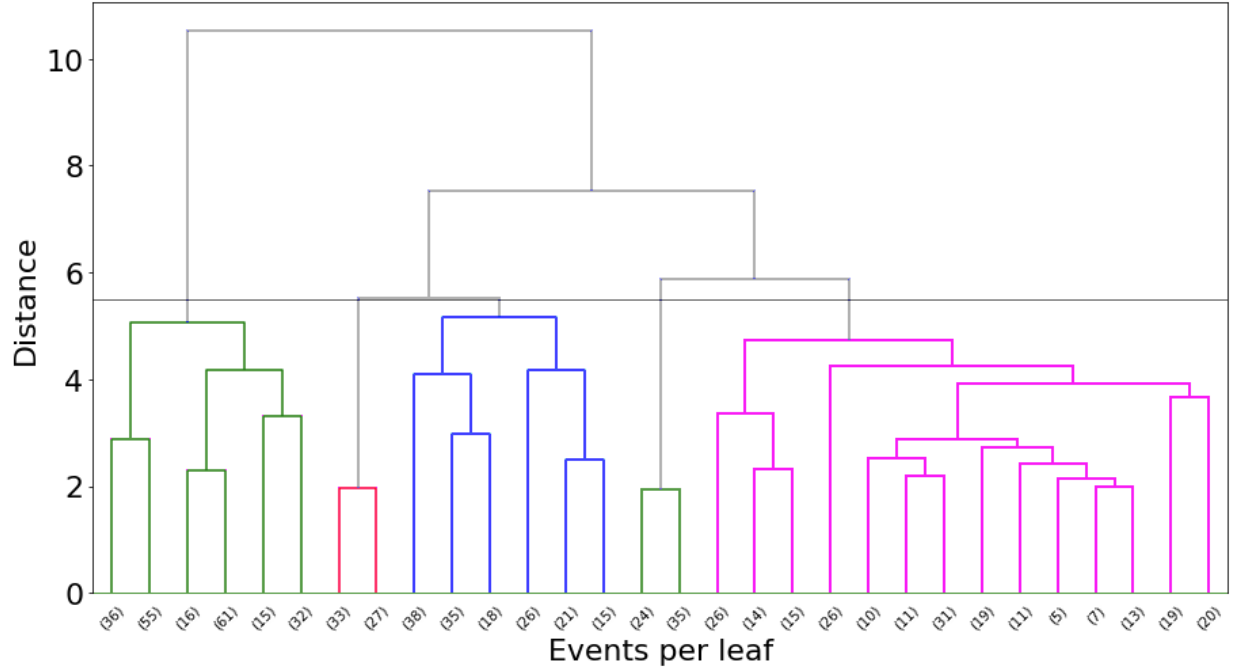


Figure S1: Dendrogram obtained from the waveform-based hierarchical clustering performed. The distance metric between two different waveforms (i and j) is estimated as $1-C_{ij}$. Ward's minimum variance linkage technique is used. The distance threshold to define the final number of cluster is set to 5.5 (the largest separation observed form dendrogram).

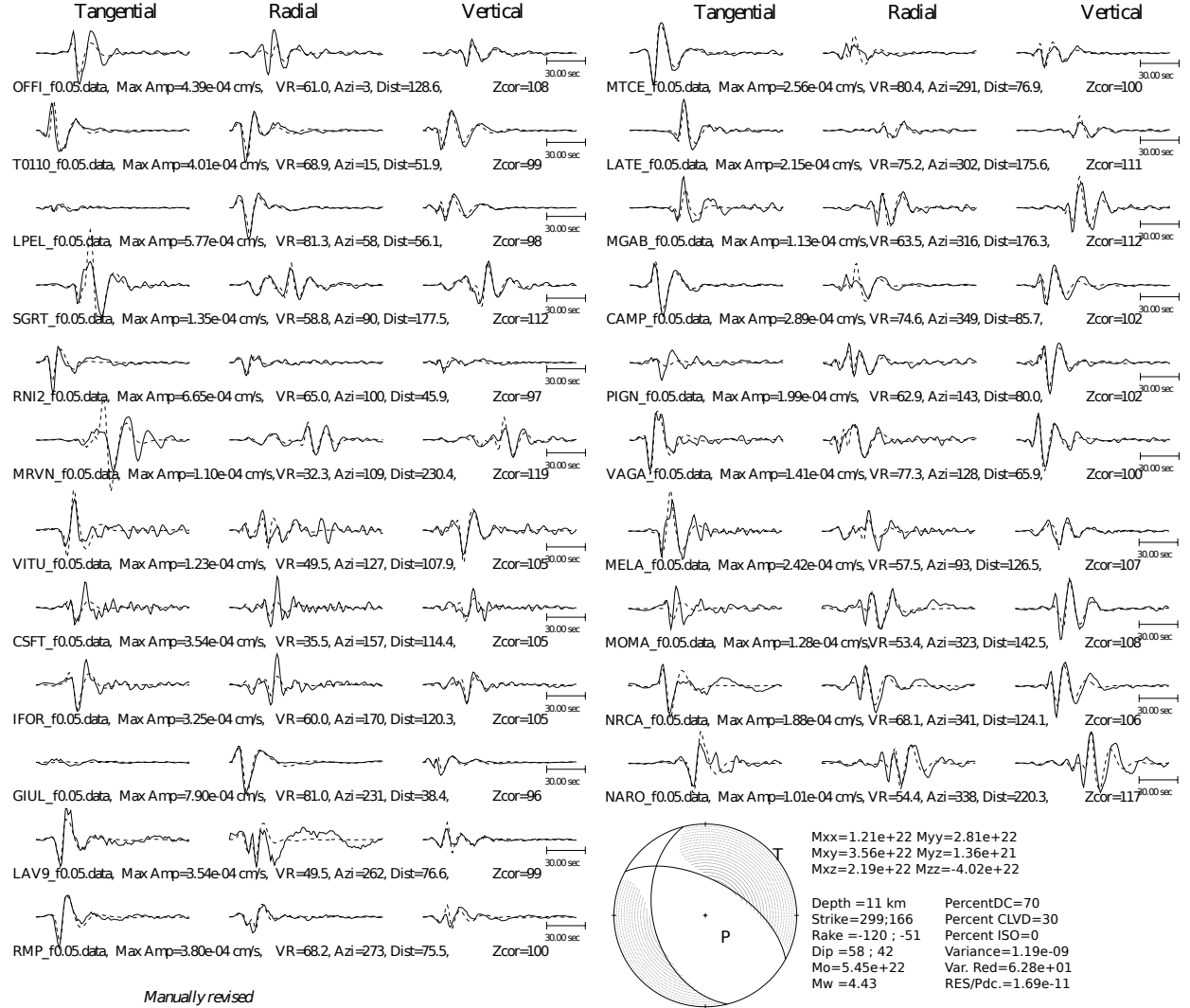


Figure S2: Estimated focal mechanism and comparison of observed (solid lines) and estimated synthetic seismograms (dashed lines) for the Mw 4.4 mainshock. The three components at 22 receiver locations are shown. This figure is a modified version from the original one provided by the INGV (http://webservices.ingv.it/webservices/ingv_ws_map/data/tdmt/15111/73711301_86_tdmt_reviewer_solution.pdf).

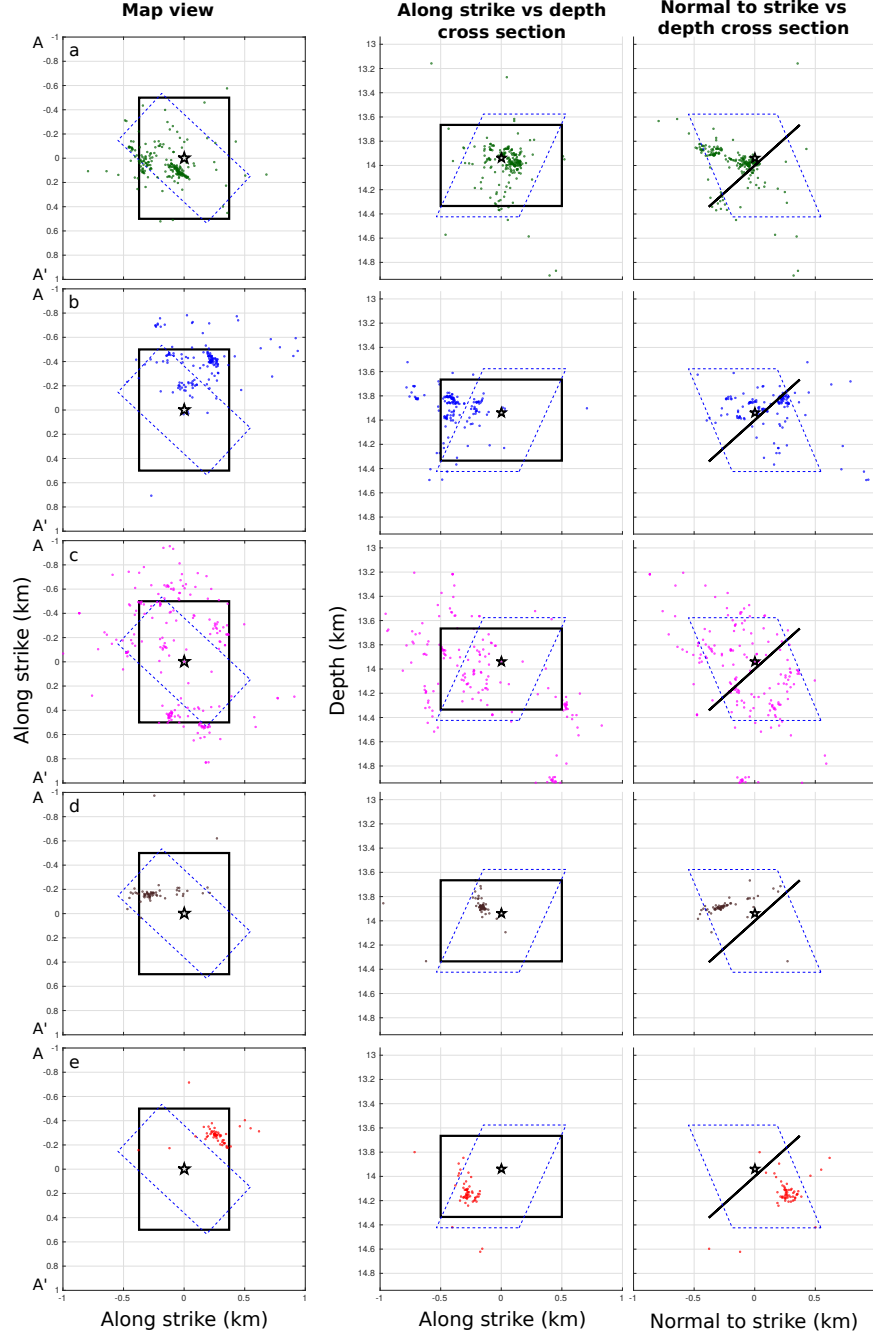
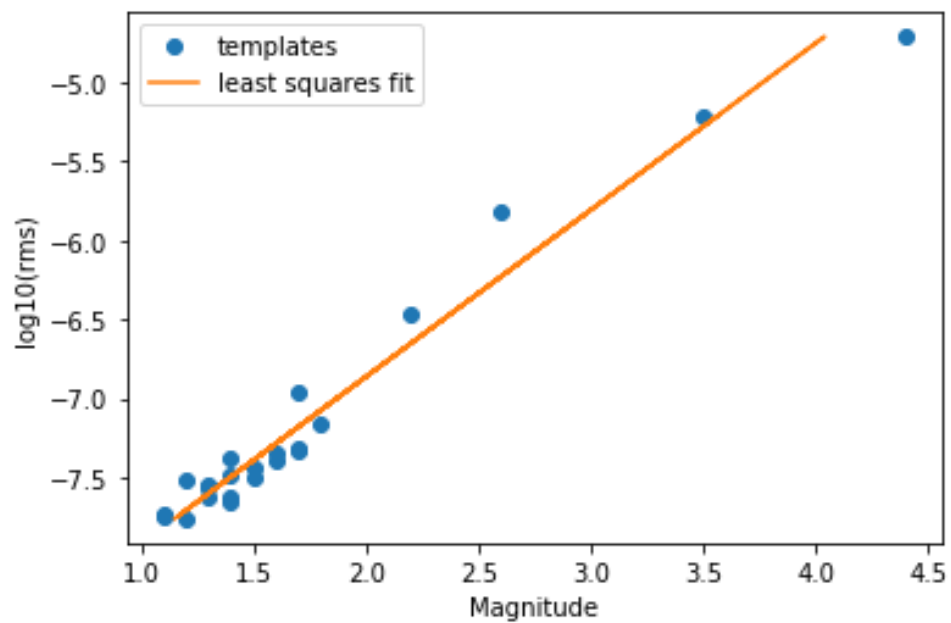
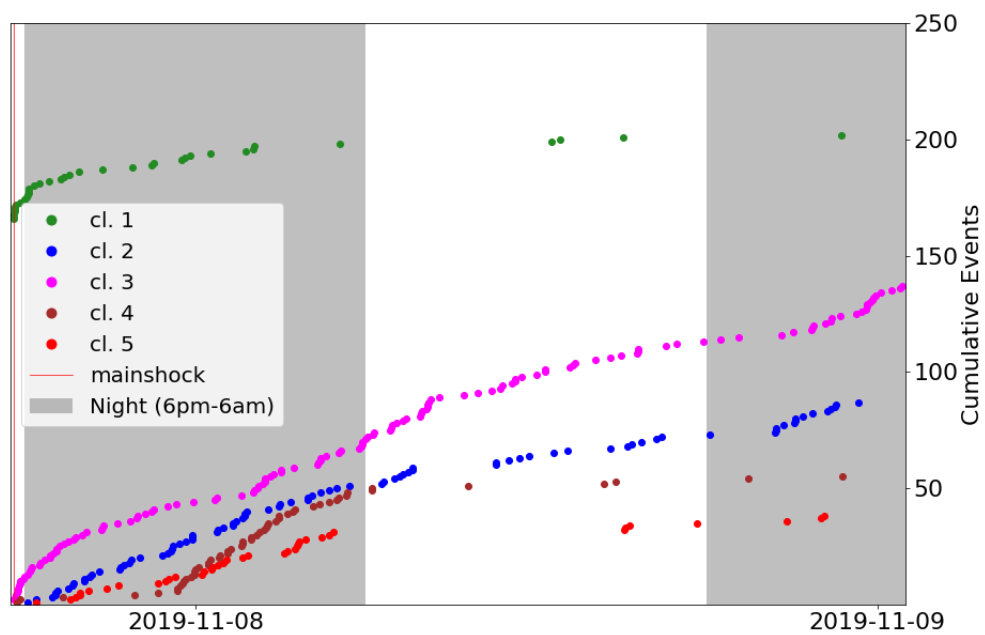


Figure S3: Map view (left column), and cross-sections along the strike (middle column) and normal-strike (right column) directions for each of the five clusters identified in the sequence (as indicated). All of the locations are relative to the mainshock hypocenter (41.7746°N 13.6066°E ; 13.94 km depth, black star). In all of the panels, the same color code is used as in Figures 3 and 4 to represent each different cluster. The solid black line represents a fault plane of 1 km^2 with the geometry of the second nodal plane (Supplementary Materials Table S1). The directions A-A' (along strike) and B-B' (normal to the strike) are the same as in Figure 1. Each cluster is represented by a corresponding label a) Cluster 1, b) Cluster 2, c) Cluster 3, d) Cluster 4 and e) Cluster 5. The blue dashed line represent the assumed auxiliary plane.



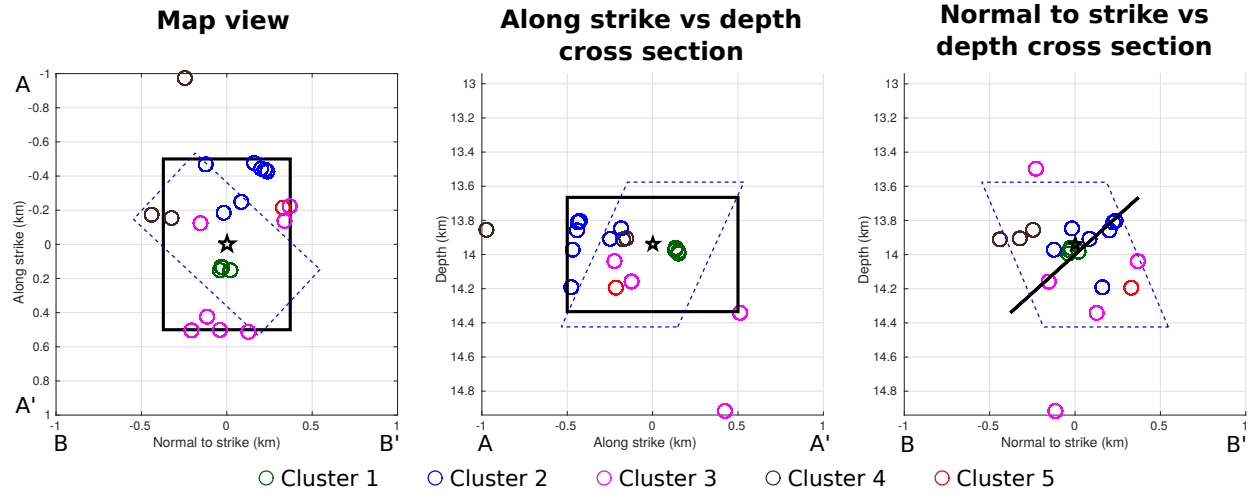


Figure S4: Map view (left), and cross-sections along the strike (middle) and normal-strike (right) directions for the assumed main fault plane (solid black line). The dashed blue line illustrates the auxiliary plane listed in Table S1 (taken from the INGV moment tensor solution). The relative location of the 23 templates used for scanning the continuous recordings are represented by the center of the colored circles. The color code used defines to which cluster each of the templates belongs to. All of the locations are relative to the mainshock hypocenter (41.7746°N 13.6066°E; 13.94 km depth, black star). The directions A-A' (along strike) and B-B' (normal to the strike) are the same as in Figure 1 in the main manuscript.

16 **References**

- 17 Bagh, S., Chiaraluce, L., De Gori, P., Moretti, M., Govoni, A., Chiarabba, C., Di Bar-
18 tolomeo, P., and Romanelli, M. (2007). Background seismicity in the central apennines
19 of italy: The abruzzo region case study. *Tectonophysics*, 444(1-4):80–92.